Differentiation of a CD4$^+$/CD8αβ$^+$ Double Positive T Cell Population From The CD8 Pool Is Sufficient To Mediate Graft-vs-Host Disease but not Graft-vs-Leukemia Effects

Nicholas J. Hess[1], David P. Turicek[1], Kalyan Nadiminti[3,5], Amy Hudson[2], Peiman Hematti[3,5], Jenny E. Gumperz[4,5], *Christian M. Capitini[1,5]

[1]Department of Pediatrics, University of Wisconsin-Madison School of Medicine and Public Health, Madison, WI
[2]Department of Microbiology and Immunology, Medical College of Wisconsin, Milwaukee, WI
[3]Division of Hematology/Oncology, Department of Medicine, University of Wisconsin-Madison School of Medicine and Public Health, Madison, WI
[4]Department of Medical Microbiology and Immunology, University of Wisconsin-Madison School of Medicine and Public Health, Madison, WI
[5]University of Wisconsin-Madison Carbone Cancer Center, Madison, WI

***Corresponding Author**:
Christian M. Capitini
University of Wisconsin
1111 Highland Ave
WIMR 4137
Madison, WI 53705
Office: (608) 262-2415
Fax: (608) 265-9721
Email: ccapitini@pediatrics.wisc.edu

ORCID: 0000-0001-5720-9305 (NJH); 0000-0003-1852-2192 (JEG); 0000-0002-2276-6731 (CMC)

Abstract Word Count = 271
Word Count = 4255
Figure Count = 7
Reference Count = 25
Running Title: DPT Are Predictive and Sufficient for GVHD

Abstract

Acute graft-vs-host disease (aGVHD) and tumor relapse remain the primary complications following allogeneic hematopoietic stem cell transplantation (allo-HSCT) for malignant blood disorders. While post-transplant cyclophosphamide has reduced the overall prevalence and severity of aGVHD, relapse rates remain a concern. Thus, there remains a need to identify the specific human T cell subsets mediating GVHD pathology versus graft-versus-leukemia (GVL) effects. In xenogeneic transplantation studies using primary human cells from a variety of donors and tissue sources, we observed the development of a mature $CD4^{+}/CD8\alpha\beta^{+}$ double positive T cell (DPT) population in mice succumbing to lethal aGVHD but not in mice that failed to develop aGVHD. The presence of DPT, irrespective of graft source, was predictive of lethal GVHD as early as one week after xenogeneic transplantation. DPT co-express the master transcription factors of the CD8 and CD4 lineages, RUNX3 and THPOK respectively, and produce both cytotoxic and modulatory cytokines. To identify the origin of DPT, we transplanted isolated human CD4 or CD8 T cells, which in turn revealed that DPT only arise from the CD8 pool. Interestingly, re-transplantation of sorted CD8 T cells from GVHD mice did not reveal a second wave of DPT differentiation. Re-transplantation of flow-sorted DPT, CD8 or CD4 T cells from GVHD mice revealed that DPT are sufficient to mediate GVHD pathology but not GVL effects versus B-cell acute lymphoblastic leukemia. Lastly, we confirmed the presence and correlation of DPT with aGVHD pathology in a small cohort of allo-HSCT patients that developed grade 2-4 aGVHD in our clinic. Further understanding of DPT differentiation and pathology may lead to targeted prophylaxis and/or treatment regimens for aGVHD and potentially other human chronic inflammatory diseases.

Key Points

1. Human DPT cell differentiation is a predictive metric of xenogeneic GVHD lethality
2. The origin of DPT are CD8 T cells that gain THPOK expression and CD4 lineage effector functions
3. DPT cells are sufficient to mediate GVHD pathology but not GVL effects

Introduction

Acute graft-vs-host disease (aGVHD) and relapse remain the primary complications following allogeneic hematopoietic stem cell transplantation (allo-HSCT)[1,2]. While the field has made significant strides in reducing aGVHD, current aGVHD prophylaxis regimens target the entire T cell population, hindering the efficacy of any graft-vs-leukemia (GVL) effects mediated by donor T cells[3,4]. Thus, delineating specific cellular mechanism(s) leading to aGVHD pathology versus GVL effects has remained a top priority for the field.

The etiology of aGVHD has been well documented using mouse models. Recipient hematopoietic and/or non-hematopoietic antigen-presenting-cells activated from the conditioning regimen present host antigen to donor T cells[5–7]. A subset of these donor T cells will be allo-reactive to the presented donor antigens and differentiate into TH_1 and $TH_{17/22}$ T cells to mediate gastrointestinal, liver and/or skin pathology[8–11]. While allo-reactive T cells are derived from both CD4 and CD8 lineages, most aGVHD research has focused on the differentiation of CD4 lineage subsets that promote pathology thought to be mediated by CD8 T cells. Unfortunately, past clinical trials investigating the inhibition of these CD4 lineages based on cytokine blockade have been met with limited success[12–14].

Recent studies have highlighted the presence of a unique human T cell population expressing both CD4 and CD8 T cell lineage markers in a variety of chronic inflammatory diseases[15–18]. These double positive T cells (DPT) have also been implicated in islet graft rejection in a nonhuman primate model[19,20]. These studies suggest that DPT may represent a novel human T cell population with a role in inflammatory diseases like aGVHD.

In this study, we identified a significant correlation between the presence of DPT in peripheral blood (PB) and aGVHD pathology. We observed in a xenogeneic transplant model that DPT were not present in any starting graft tissue, developed only after transplantation and were significantly correlated and predictive of lethal aGVHD. DPT differentiated from the CD8 T cell pool and gained expression of the master CD4 transcription factor, THPOK, along with the capacity to secrete modulatory cytokines normally associated with the CD4 lineage. Isolated DPT were sufficient to mediate aGVHD pathology but had no direct GVL activity against two human B-cell acute lymphoblastic leukemia (B-ALL) cell lines. Lastly, we collected leftover blood samples from non-GVHD and grade 2-4 aGVHD allo-HSCT patients and confirmed the presence and correlation of DPT with aGVHD diagnosis.

Methods

Isolation of Primary Human Cells. Human peripheral blood was collected from healthy consenting donors according to IRB protocol 2014-0806. Leftover and de-identified remnants of human bone marrow and G-CSF mobilized peripheral blood grafts used for allo-HSCT procedures were collected under IRB protocol 2016-0298. De-identified human umbilical cord blood was collected from the Medical College of Wisconsin's cord blood bank. All human blood samples were diluted 1:1 with leukocyte isolation buffer, composed of phosphate-buffered saline (PBS), 2mM EDTA and 2% fetal bovine serum (FBS), prior to ficoll density-gradient centrifugation (1100xg for 15 min with 0 brake). When indicated, RosetteSep T cell, CD4 or CD8 enrichment kits were used (STEMCELL Technologies, Seattle, WA). For Figure 4F and Figure 7, leftover primary human blood samples were collected from allo-HSCT patients according to IRB protocol 2020-1490. RBC were lysed using 1X RBC lysis buffer (BioLegend) and stained for flow cytometry.

Transplantation of human cells into NBSGW Mice. Equal numbers of male and female immunodeficient NSG (NOD.Cg-*Prkdc*^{scid} *Il2rg*^{tm1Wjl}/SzJ, Jackson Laboratories, Bar Harbor, ME) or NBSGW (NOD.Cg-Kit^{W41J}Tyr^{+}Prkdc^{scid}IL2rg^{tm1Wjl}/ThomJ) between the ages of 8-16 weeks of age were used for all experiments. All human cells were washed and resuspended in 150µL/mouse of sterile 1X PBS prior to retro-orbital injection. All mice were weighed and monitored weekly for visible signs of GVHD with a scoring system carried out as follows: 0 = no signs of GVHD; 1 = 2-5% weight loss; 2 = 6-9% weight loss; 3 = 10-14% weight loss; 4 = ≥ 15% weight loss. Blood was regularly drawn at 1, 3, 6, 9- and 12-weeks post-transplant by retro-orbital bleeding. At time of euthanasia, the spleen, one lobe of the liver, lungs and femur were collected for further processing. All tissue processing and H&E staining was performed by the Experimental Animal Pathology Lab at the University of Wisconsin-Madison.

Flow Cytometry and Cell-Sorting. All cells were stained in flow buffer (PBS, 10% FBS) prior to quantification on an Attune NxT Flow Cytometer (ThermoFisher, Carlsbad, CA) and analysis on FlowJo v10 (Ashland, OR). For intracellular cytokine staining, Brefeldin A (BioLegend) was added ~4hrs prior to staining. Fixation buffer was added to the cells prior to intracellular staining permeabilization wash buffer (BioLegend) and antibody staining. The antibody clones used include mCD45 (A20), ICOS (C398.4A), T-bet (4B10), LAG3 (11C3C65), FASL (NOK-1), CD4 (OKT4), CD69 (FN50), OX40 (Ber-ACT35), CD27 (O323), pSTAT4 (p38), RORγt (Q21-559), CD44 (BJ18), NKG2D (1D11), PD-1 (EH12.2H7), THPOK (ZFP-67), TIGIT (A15153G), CD45RO (UCHL1), TIM3 (F38-2E2), pSTAT1 (A17012A), pSTAT3 (13A3-1), pSTAT6 (A15137E), IL-22

(2G12A41), GATA3 (16E10A23), CD8α (RPA-T8), CD25 (BC96), BCL2 (100) 4-1BB (4B4-1), CD28 (CD28.2), CTLA4 (BNI3), PanHLA (w6/32), CD3 (UCHT1), RUNX3 (SD0803 - ThermoFisher) and CD8β (SIDI8BEE - ThermoFisher). All antibody clones were from BioLegend unless otherwise stated. Visualization of cells was complete using an ImageStream Mark II (EMD Millipore, Burlington, MA).

For cell sorting, cells were collected from the blood, spleen, liver, and lungs of mice transplanted with a lethal dose of PB-mononuclear cells (MNC) approximately 4 weeks prior. Processed tissues were ficolled as described above to obtain PB-MNC. Human cells were isolated from the combined PB-MNC using an EasySep Mouse/Human Chimera isolation kit (STEMCELL Technologies). Human cells were then stained in sterile PBS with the human CD4 (OKT4) and CD8β (SIDI8BEE) antibodies prior to sorting on a FACSAria Cell Sorter (BD Biosciences, San Jose, CA). Cells were then maintained in cell culture for 2-3 days prior to transplantation and/or expansion.

Cell Lines and Cell Culture. The human B-ALL cell lines RS4;11 and NALM-6 were purchased from ATCC (Manassas, VA) and cultured using standard RPMI-10 media (RPMI base media, 10% FBS, 1X Pen/Strep, 1mM NEAA, 1X GlutaMAX - ThermoFisher). All cell lines were mycoplasma tested and authenticated prior to use (IDEXX Bioresearch, Westbrook, ME). After flow sorting, isolated human CD4, CD8 and DPT populations were expanded by co-culturing with a 10X dose of irradiated (25Gy, XRAD320 x-ray irradiator) human mononuclear cells from a third-party donor with 5μg/mL PHA (Millipore Sigma) in RPMI-10 media supplemented with 5ng/mL of recombinant human IL-2 (NCI Biological Resources Branch, Frederick, MD) and IL-7 (Peprotech). RPMI-10 media supplemented with IL-2 and IL-7 was exchanged approximately every 3-4 days.

ELISAs. Mouse blood samples were diluted with 50μL of 1X PBS prior to centrifugation with 60μL of diluted plasma stored at -20^{0}C. Plasma was further diluted 1:5 prior to ELISA with Assay Buffer (PBS, 1mM Tween-20, 5% FBS). IFNγ ELISAs used the MD-1 clone for coating and a biotinylated 4S.B3 clone for detection prior to visualization with a streptavidin-HRP antibody (BioLegend).

Metabolomic Assay. ATP production rate was calculated from flow sorted CD4, CD8 and DPT using an Seahorse XF Real-Time ATP Rate Assay Kit (Agilent, Santa Clara, CA) on a Seahorse XF/XFe96 analyzer (Agilent) following the manufacturer's instructions.

Bioluminescent Imaging. A total of $1E^6$ luciferase positive NALM-6 cells were injected retro-orbitally seven days prior to human T cell transplantation as described above. Luminescence detection was gathered at the indicated times using an IVIS Spectrum In Vivo Imaging System (PerkinElmer, Waltham, MA). Briefly, mice were anesthetized and intraperitoneally injected with 100µL of D-luciferin at 30mg/mL and measured for bioluminescence approximately 15 minutes later.

Statistics. Graphs and statistical tests were completed using Prism v6 (GraphPad Software, San Diego, CA). Comparison of 2 groups of data were performed using either unpaired parametric (for linear data) or non-parametric (for logarithmic data) t-tests. A log rank analysis was used for all survival data. A p value less than 0.05 was considered significant.

Study Approval. Human cells and tissues were obtained under IRB protocol 2014-0806 (CMC), 2016-0298 (PH), and 2020-1490 (CMC). Mice procurement and experiments were performed at the University of Wisconsin-Madison under IACUC approved animal protocol M005915-R01 (CMC).

Results

DPT development after transplantation is predictive of lethal GVHD in a xenogeneic transplant model.

Despite the intensive research on aGVHD using mouse models, the number of studies directly investigating capacity of human T cell subsets to mediate pathology remains limited. This study sought to how human T cell subsets mediated pathology in a non-conditioned xenogeneic transplant model. We have previously shown that the development of lethal GVHD in this model system is not inevitable and in fact can be modulated based on a variety of biological variables[21]. Surprisingly, transplanting either human PB-MNC or isolated human peripheral blood T cells (PB-Tc) at sub LD_{100} doses, revealed the presence of a human T cell population expressing both CD4 and CD8 preferentially in mice developing lethal GVHD (Figure 1A-C). These double positive T cells (DPT) express both CD8α and CD8β and develop irrespective of the human graft tissue used (Figure 1D, Supplemental Figure 1). The presence of DPT was detected as early as 1-week post-transplant and across multiple xenogeneic GVHD target organs at the time of sacrifice (Figure 1C-D, Supplemental Figure 2). Interestingly, the percentage of DPT in the blood of mice at 1-, 3- and 6-weeks post-transplant was highly predictive of lethal GVHD development in this model system (Figure 1E). Lastly, DPT were confirmed to represent a mature human T cell population in this model based on singlet flow cytometric gating, Imagestream analysis and the universal expression of CD45RO, an antigen-experienced marker, on the DPT population (Figure 1F). While this unique T cell population has been identified in other human chronic inflammatory diseases, a detailed understanding of their origin and function had remained unexplored until now[15–20].

DPT arise from highly activated CD8 T cell clones

Unsupervised tSNE clustering of eight T cell markers demonstrated that DPT were more closely related to the CD8 population than CD4 (Figure 2A). To definitively determine the origin of the DPT population, we transplanted isolated CD4 or CD8 T cells from the peripheral blood of healthy donors into a xenogeneic transplant model and monitored the mice for the development of DPT. Interestingly, DPT only developed from CD8 T cells but not CD4 T cells (Figure 2B-C). Furthermore, re-transplantation of flow-sorted CD8 T cells did not result in a second wave of DPT differentiation suggesting that DPT differentiate from specific clones within the CD8 population (Figure 2D-F). Additional analysis of the phospho-STAT repertoire between the CD8 and DPT populations did not reveal any significant differences, suggesting that cytokines may not drive

differentiation of DPT from the CD8 population (Supplemental Figure 3).

Expression of CD4 on DPT coincides with the master transcription factor THPOK

During T cell development in the thymus, the master transcription factors RUNX3 and THPOK are co-expressed until lineage identity (marked by TCR reactivity to either MHC class-I or -II) is determined. Afterwards, the dominant transcription factor, RUNX3 for CD8 T cells and THPOK for CD4 T cells, conserve lineage identification through the negative regulation of their counterpart (Figure 3A)[22]. Surprisingly, DPT express both RUNX3 and THPOK concomitantly, though at intermediate expression levels, compared to single positive CD4 and CD8 T cell controls (Figure 3B-C). Using CD4 expression as a surrogate for THPOK expression, we next determined if the expression of CD4 is conserved overtime. Flow-sorted DPT were either re-stimulated ex vivo with irradiated human PB-MNC and PHA or re-transplanted back into naïve NSG mice to determine if an in vivo immune milieu is required to maintain CD4 expression on DPT. Most of the flow sorted DPT were able to maintain their expression of CD4 by either stimulation method for up to 21 days ex vivo or 63 days in vivo (Supplemental Figure 4).

DPT repertoire of co-stimulatory and inhibitory ligands are expressed at intermediate levels compared to single positive CD8 and CD4 populations

The CD8 and CD4 T cells display lineage specific expression differences in their co-stimulatory and co-inhibitory receptors. Since DPT expressed both RUNX3 and THPOK, we next determined if this resulted in functional changes in their co-stimulatory and co-inhibitory expression patterns. Similar to CD8 T cells, DPT displayed high levels of NKG2D, and all T cell populations exhibited high levels of CD44 as expected when present in a lymphopenic environment (Figure 3E-F). But while CD8 T cells have high levels of CD27 and ICOS, DPT has significantly lower levels of these markers, yet still slightly higher than CD4 T cells (Figure 3F). Conversely, CD4 T cells displayed high levels of OX40, with DPT having slightly lower levels but still significantly higher than CD8 T cells (Figure 3F). The same phenomenon was detected with several co-inhibitory receptors such as LAG3, TIGIT and TIM3, which were all high on CD8 T cells and DPT but not on CD4 T cells. Meanwhile PD-1 expression was highest on CD4 T cells, intermediate on DPT and lowest on CD8 T cells (Figure 3G). These same expression patterns were detected in the spleen of GVHD mice and after ex vivo stimulation of flow-sorted T cell populations (Supplemental Figure 5A-B).

The DPT population is highly activated and secrete both cytotoxic and modulatory cytokines

Due to the co-expression of the CD8 and CD4 lineage-specific transcription factors and co-stimulatory/inhibitory receptors, we sought to investigate if the DPT population can secrete both CD8 and CD4 lineage-specific cytokines. T cells taken from the blood of GVHD mice were cultured overnight with PMA/ionomycin to characterize their secretome. Interestingly, our results revealed that DPT were able to secrete not only granzyme and perforin, but also IFNγ, TNFα, IL17A, IL22 and GM-CSF which are normally reserved for the CD4 lineage (Figure 4A). Surprisingly, this same expression pattern was seen when T cells were cultured overnight without a stimulator (only brefeldin A), suggesting that DPT can not only secrete a broad repertoire of cytokines, but are also actively producing these cytokines in vivo (Figure 4B, Supplemental Figure 6). In support of this observation, we have also detected that DPT express the transcription factors T-bet and RORγt at intermediate levels compared to single-positive T cell controls (Supplemental Figure 5C-E).

To further demonstrate DPT are a highly activated T cell population, we performed a metabolic analysis of overall ATP production rate and relevant contribution from the glycolytic and oxidative pathways. While all T cell populations displayed similar levels of oxidative respiration, the DPT population had increased ATP production from the glycolytic pathway, which has been shown to be associated with T cell activation (Figure 4C). T cell blasting is another example of highly activated and proliferative T cells that is observed through the increase in their overall size as a precursor for cell division. While all T cell populations exhibited blasting, a significantly higher proportion of the DPT population was blasting compared to the CD8 population across several different tissues (Figure 4D-E). Furthermore, we compared the blasting percentages of CD4, CD8 and DPT in five primary aGVHD patient samples, which again revealed that a higher proportion of DPT are blasting compared to CD4 and CD8 single positive cells (Figure 4F).

DPT are sufficient for GVHD pathology

Since we have shown that the DPT population represents a highly activated T cell population in GVHD, we next sought to confirm if DPT are required and sufficient for GVHD pathology. First, we transplanted isolated CD4 and CD8 T cells from the blood of healthy donors and monitored the mice for survival. Both the CD4 and CD8 T cell populations were able to mediate GVHD, though much higher doses were required for this to occur (i.e., $1E^7$ CD4/CD8 T cells vs $2E^6$ CD3 T cells) (Figure 5A-D and Figure 1B). Importantly, since DPT developed when isolated CD8 T cells were transplanted, we next re-transplanted flow sorted DPT, CD4 and CD8 T cells from several GVHD mice into naïve mice and monitored for survival. This experiment showed that at

the lower cell doses (i.e., $3E^6$), the DPT population was able to mediate lethal GVHD while the CD8 population, which did not re-develop a second wave of DPT, was unable to cause GVHD (Figure 5E-G and Figure 2E-F). The DPT were shown to have increased systemic IFNγ levels in the plasma and increased T cell infiltration in a variety of organs (Figure 5H-K).

DPT cannot mediate GVL activity against human B-ALL

We have shown that DPT represent highly activated T cell population arising from the CD8 T cell pool and are sufficient for GVHD pathology, but it is currently unclear if they can mediate a GVL effect. To test this, we transplanted the human B-ALL cancer line RS4;11 seven days prior to the transplantation of isolated DPT or human PB-MNC. Mice from all groups died between four and ten weeks after transplantation, though while the PB-MNC group exhibited classical signs of GVHD, mice transplanted with DPT showed pathology similar to the no treatment (NT) group (Figure 6A). Flow cytometric analysis revealed that while the RS4;11 cancer line remained abundant in the mice given DPT, the B-ALL cells were almost undetectable in mice given PB-MNC (Figure 6B-C). The striking difference in GVL activity was not due to the lack of T cells, with both groups exhibiting an expansion of T cells in their blood over time and increasing levels of IFNγ in the serum (Figure 6D-E). PB-MNC mice experienced a more robust expansion of T cells expansion and IFNγ production, which may be the result of having synergy from both CD4 and CD8 T cells present.

To control for this, we next transplanted isolated CD4 or CD8 T cells from healthy donors into an NSG mouse previously transplanted with the more aggressive NALM-6 human B-ALL cancer line in addition to DPT. All mice succumbed to leukemia although mice transplanted with CD4 or CD8 T cells experienced significantly prolonged survival (Figure 6F). This prolonged survival was most likely the result of delayed leukemia progression as detected by IVIS and flow cytometry (Figure 6G-I). Importantly though, there was no difference in T cell expansion in vivo suggesting that the enhanced GVL activity in single-positive CD4 and CD8 T cells was not due to overall higher T cell numbers (Figure 6J). Furthermore, we did not detect any additional DPT differentiation from the CD8 pool as a result of GVL activity (data not shown). Lastly, CD4 and CD8 T cells flow sorted from GVHD mice also had enhanced GVL activity compared to DPT, though their overall GVL activity was slightly diminished (Supplemental Figure 7). Overall, we have identified a unique human T cell subset characterized by co-expression of CD4 and CD8αβ as well as the transcription factors RUNX3 and THPOK that is associated with the presence of severe aGVHD. This DPT population differentiates from the CD8 T cell pool, exhibits a highly inflammatory

phenotype and is sufficient to mediate GVHD pathology. Despite their inflammatory profile, DPT do not mediate a GVL effect against B-ALL and may represent a biomarker that can distinguish aGVHD from GVL.

Clinical aGVHD is correlated with increased DPT frequency.

To confirm the association between DPT and aGVHD we have identified in our xenogeneic transplant model, we collected leftover blood samples from 27 allo-HSCT patients between 70-90 post-transplant. Of these 27 patients, 14 had never developed aGVHD pathology while the other 13 had active aGVHD of grade 2 or greater. Analysis of their blood samples revealed a higher percentage of DPT in the patients with active grade 2 or higher aGVHD compared to the non-aGVHD controls (Figure 7).

Discussion

In this study, we highlight the GVHD-specific activity of a human DPT population that differentiates from the CD8 population as a result of antigen-stimulation. DPT have been identified in renal cell carcinoma, β-thalassemia major, rheumatoid arthritis and even in allo-HSCT patients[15–18]. DPT have also been implicated in islet graft rejection in a nonhuman primate model, suggesting that DPT are an important differentiation state of human T cells[19,20].

One unique feature of DPT is their co-expression of the CD8 and CD4 lineage master transcription factors, RUNX3 and THPOK respectively. While the co-expression of these transcription factors is normally reserved for T cell development in the thymus, one other study using a xenogeneic transplant model has shown that mature human T cells can co-express these transcription factors[18,22]. Naturally, one assumption is that we are observing a variation of de novo T cell development in our model system. To account for this, we primarily used PB-MNC grafts which have extremely low levels of hematopoietic stem cells (<0.1%)[23,24]. Additionally, we confirmed that DPT do not express CD31, a marker of recent thymic emigrants and are positive for the antigen-experienced marker CD45RO[21]. Lastly, NSG mice lack a functional thymus to support de novo T cell development, which, in addition to our data showing that DPT are single cells, provides strong evidence that DPT are a fully mature human T cell population.

The specific cellular signals on CD8 T cells that initiate DPT differentiation is currently not known, though our data supports the hypothesis that it is the result of chronic antigen exposure. Since we did not detect a second wave of DPT differentiation after the re-transplantation of sorted CD8 T cells from GVHD mice, we assume that the remaining CD8 T cell clones are incapable of responding to murine tissue antigens. While the specific signals for DPT differentiation are unknown at this time, we can assume that there is little/no involvement of pro-inflammatory cytokines based on our use of non-conditioned NSG mice and lack of increased phospho-STAT expression in DPT[21,23]. While not directly investigated, non-conditioned NSG mice do not develop a “cytokine storm” as a result of γ-irradiation with the levels of pro-inflammatory cytokines in non-conditioned mice thought to be extremely low. Unfortunately, other than CD28:CD80/CD86 axis which is known to be cross-reactive between human and mice, there is little information on the cross-reactivity of the other co-stimulatory proteins[23].

The identification of DPT as a highly reactive T cell subset also provides additional insight into the mechanism of PTCy mediated GVHD suppression. PTCy is thought to eliminate rapidly

dividing T cells (i.e. antigen activated T cells) through the cross-linking of DNA by its metabolite phosphoramide that leads to apoptosis[25]. It is thought that slowly dividing T cell clones maintain high enough concentration of the protein aldehyde dehydrogenase to protest themselves from PTCy induced apoptosis, thus eliminating the majority of T cell clones capable of causing GVHD[25]. Since we know that DPT are a highly activated T cell population, one interesting hypothesis is that PTCy also acts by eliminating DPTs. Unfortunately, while this may be true, PTCy also has the "side-effect" of removing GVL-specific T cell clones. Thus, if the above hypothesis is proven true, the targeted elimination of DPT, which we have observed to not have any direct GVL activity against at least B-ALL (Figure 7), may become a more specific and directed GVHD prophylaxis regimen in the future. Testing of DPT against other hematologic malignancies in vitro and with in vivo GVL models will be warranted.

In summary, we have identified a unique human $CD4^+/CD8\alpha\beta^+$ DPT cell population that is not present in healthy human graft tissues, differentiates from the CD8 T cell population after xenogeneic and clinical allo-HSCT, and is predictive of GVHD lethality in mice. DPT are highly reactive CD8 T cell clones that gain expression of THPOK and subsequent CD4 lineage effector functions. Furthermore, when isolated DPT are transplanted into NSG mice, the DPT population is sufficient to mediate GVHD pathology but does not mediate GVL activity against human B-ALL cell lines. Overall, the identification of DPT as a GVHD-specific T cell population in allo-HSCT recipients serves as validation of the cellular T cell responses observed post-transplant in xenogeneic transplant models. Future studies will need to determine if measurement of DPT prospectively may help predict development of aGVHD and if targeting and/or preventing DPT differentiation may suppress GVHD.

Author Contributions

NJH, JEG and CMC designed the study; NJH and DPT performed experiments; NJH analyzed the data; AWH and PH provided resources; NJH and CMC wrote and edited the manuscript.

Acknowledgements

The authors would like to thank the University of Wisconsin Carbone Cancer Center (UWCCC) Flow Cytometry Laboratory, UWCCC Small Molecule Screening Facility, UWCCC Small Animal Imaging and Radiotherapy Facility and UWCCC Experimental Animal Pathology Laboratory, who are supported in part by NIH/NCI P30 CA014520.

Grant Support

This work was supported in part by NIH/NIAID T32 AI125231 (N.J.H), NIH/NHBLI T32 HL07899 (N.J.H.), NIH/NCATS UL1 TR002373 (N.J.H), the Cormac Pediatric Leukemia Fellowship (N.J.H) and the Stem Cell and Regenerative Medicine Center Fellowship (N.J.H.). Additional funding includes NIH/NIAID R21 AI105841, NIH/NIAID R21 AI116007 (J.E.G.), NIH/NIAID R01 AI136500 (J.E.G.), NIH/NHLBI R01 HL153721 (P.H. and C.M.C), St. Baldrick's-Stand Up to Cancer Pediatric Dream Team Translational Research Grant SU2C-AACR-DT-27-17 (C.M.C.), American Cancer Society Research Scholar grant RSG-18-104-01-LIB (C.M.C.), NIH/NCI R01 CA215461 (C.M.C.), and the Midwest Athletes Against Childhood Cancer (MACC) Fund (C.M.C). The St. Baldrick's Foundation collaborates with Stand Up To Cancer. Stand Up To Cancer is a division of the Entertainment Industry Foundation. Research grants are administered by the American Association for Cancer Research, the scientific partner of SU2C. The contents of this article do not necessarily reflect the views or policies of the Department of Health and Human Services, nor does mention of trade names, commercial products, or organizations imply endorsement by the US Government. None of these funding sources had any input in the study design, analysis, manuscript preparation or decision to submit for publication.

Disclosure of Conflicts of Interest

C.M.C. reports honorarium from Nektar Therapeutics and Novartis, who had no input in the study design, analysis, manuscript preparation or decision to submit for publication. The authors declare that no other relevant financial conflicts of interest exist.

References

1. D'Souza A, Fretham C, Lee SJ, et al. Current Use of and Trends in Hematopoietic Cell Transplantation in the United States. *Biol Blood Marrow Transplant*. 2020;26(8):e177–e182.
2. Gooptu M, Romee R, St Martin A, et al. HLA-haploidentical vs matched unrelated donor transplants with posttransplant cyclophosphamide-based prophylaxis. *Blood*. 2021;138(3):273–282.
3. Martinez-Cibrian N, Zeiser R, Perez-Simon JA. Graft-versus-host disease prophylaxis: Pathophysiology-based review on current approaches and future directions. *Blood Reviews*. 2020;100792.
4. Chang Y-J, Zhao X-Y, Huang X-J. Strategies for Enhancing and Preserving Anti-leukemia Effects Without Aggravating Graft-Versus-Host Disease. *Front Immunol*. 2018;9:3041.
5. Piper C, Zhou V, Komorowski R, et al. Pathogenic Bhlhe40+ GM-CSF+ CD4+ T Cells Promote Indirect Alloantigen Presentation in the GI Tract during GVHD. *Blood*. 2019;
6. Koyama M, Kuns RD, Olver SD, et al. Recipient nonhematopoietic antigen-presenting cells are sufficient to induce lethal acute graft-versus-host disease. *Nat. Med.* 2011;18(1):135–142.
7. Koyama M, Mukhopadhyay P, Schuster IS, et al. MHC Class II Antigen Presentation by the Intestinal Epithelium Initiates Graft-versus-Host Disease and Is Influenced by the Microbiota. *Immunity*. 2019;
8. Gartlan KH, Koyama M, Lineburg KE, et al. Donor T-cell-derived GM-CSF drives alloantigen presentation by dendritic cells in the gastrointestinal tract. *Blood Adv*. 2019;3(19):2859–2865.
9. Park S, Griesenauer B, Jiang H, et al. Granzyme A-producing T helper cells are critical for acute graft-versus-host disease. *JCI Insight*. 2020;
10. Hashimoto K, Kouno T, Ikawa T, et al. Single-cell transcriptomics reveals expansion of cytotoxic CD4 T cells in supercentenarians. *Proc Natl Acad Sci U S A*. 2019;116(48):24242–24251.
11. Kim S, Reddy P. Targeting Signal 3 Extracellularly and Intracellularly in Graft-Versus-Host Disease. *Front Immunol*. 2020;11:722.
12. Kennedy G, Tey S-K, Buizen L, et al. A Phase 3 Double-Blind Study of the Addition of Tocilizumab versus Placebo to Cyclosporin/Methotrexate GvHD Prophylaxis. *Blood*. 2021;
13. Antin JH, Weisdorf D, Neuberg D, et al. Interleukin-1 blockade does not prevent acute graft-versus-host disease: results of a randomized, double-blind, placebo-controlled trial of interleukin-1 receptor antagonist in allogeneic bone marrow transplantation. *Blood*. 2002;100(10):3479–3482.
14. Locke FL, Pidala J, Storer B, et al. CD25 Blockade Delays Regulatory T Cell Reconstitution and Does Not Prevent Graft-versus-Host Disease After Allogeneic Hematopoietic Cell Transplantation. *Biol Blood Marrow Transplant*. 2017;23(3):405–411.
15. Menard LC, Fischer P, Kakrecha B, et al. Renal Cell Carcinoma (RCC) Tumors Display Large Expansion of Double Positive (DP) CD4+CD8+ T Cells With Expression of Exhaustion Markers. *Front Immunol*. 2018;9:2728.
16. Zahran AM, Saad K, Elsayh KI, Alblihed MA. Characterization of circulating CD4+ CD8+ double positive and CD4- CD8- double negative T-lymphocyte in children with β-thalassemia major. *Int. J. Hematol.* 2017;105(3):265–271.
17. Quandt D, Rothe K, Scholz R, Baerwald CW, Wagner U. Peripheral CD4CD8 double positive T cells with a distinct helper cytokine profile are increased in rheumatoid arthritis. *PLoS ONE*. 2014;9(3):e93293.
18. Alhaj Hussen K, Michonneau D, Biajoux V, et al. CD4+CD8+ T-Lymphocytes in Xenogeneic and Human Graft-versus-Host Disease. *Front Immunol*. 2020;11:579776.
19. Choi YJ, Park H-J, Park HJ, Jung KC, Lee J-I. CD4hiCD8low Double-Positive T Cells Are Associated with Graft Rejection in a Nonhuman Primate Model of Islet Transplantation. *J Immunol Res*. 2018;2018:3861079.

20. Overgaard NH, Jung J-W, Steptoe RJ, Wells JW. CD4+/CD8+ double-positive T cells: more than just a developmental stage? *J. Leukoc. Biol.* 2015;97(1):31–38.
21. Hess NJ, Hudson AW, Hematti P, Gumperz JE. Early T Cell Activation Metrics Predict Graft-versus-Host Disease in a Humanized Mouse Model of Hematopoietic Stem Cell Transplantation. *J. Immunol.* 2020;205(1):272–281.
22. Egawa T. A Fateful Decision in the Thymus Controlled by the Transcription Factor ThPOK. *J.I.* 2021;206(9):1981–1982.
23. Hess NJ, Brown ME, Capitini CM. GVHD Pathogenesis, Prevention and Treatment: Lessons From Humanized Mouse Transplant Models. *Frontiers in Immunology*. 2021;12:3082.
24. Hess NJ, Lindner PN, Vazquez J, et al. Different Human Immune Lineage Compositions Are Generated in Non-Conditioned NBSGW Mice Depending on HSPC Source. *Front Immunol*. 2020;11:573406.
25. Nunes NS, Kanakry CG. Mechanisms of Graft-versus-Host Disease Prevention by Post-transplantation Cyclophosphamide: An Evolving Understanding. *Front Immunol*. 2019;10:2668.

Figure Legends

Figure 1. Development of DPT after transplant is predictive of GVHD lethality.

(A-B) Kaplan-Meier survival curve of NSG mice transplanted with $5E^6$ PB-MNC (A) or $2E^6$ PB-Tc (B). Representative dot plots of mouse blood at 3 weeks post-transplant from a mouse that did not develop GVHD (blue mouse) and a mouse that died of GVHD (red mouse) highlighting the presence of DP T cells (red box). Dot plots were gated upstream on singlets, human panHLA-I and CD3. (C-D) Bar graph showing the percentage of DP T cells at 1-, 3- and 6-weeks post-transplant in mice transplanted with PB-MNC (C) and at 1-week post-transplant in mice transplanted with the mononuclear fraction of the graft source indicated. Each dot represents an individual mouse taken from 5 independent experiments. (E) Receiver-operator-characteristic (ROC) curve showing the predictive value of DP T cells. (F) Representative Imagestream analysis of human T cell isolated from mouse blood at 3-weeks post-transplant. PB (peripheral blood), MB (G-CSF mobilized peripheral blood), BM (bone marrow), CB (umbilical cord blood), MNC (mononuclear cells), allo-HSCT (allogeneic hematopoietic stem cell transplant). * $p<0.05$, ** $p<.01$, *** $p<0.001$

Figure 2. DPT differentiate from highly reactive CD8 clones.

(A) Unsupervised tSNE clustering of human T cells concatenated from five GVHD mice. (B-C) Freshly isolated CD3, CD4 and CD8 PB-T cells from a healthy donor were transplanted into non-irradiated NSG mice. Representative dot plots show the percentage of DP T cells in the mouse blood at 3-weeks post-transplant (B) with the percentage of DP T cells from isolated CD4 and CD8 T cells transplantation further quantified (C). (D-F) NSG mice transplanted with PB-MNC for 4 weeks were euthanized and their organs harvested, ficolled, human cell isolated by magnetic isolation and the CD4 and CD8 T cells flow-sorted (D). (E) Dot plot highlighting the percentage of DP T cells in the blood of mice transplanted with flow-sorted CD4 and CD8 T cells 3-weeks post-transplant. (F) Further quantification of (E). * $p<0.05$, ** $p<.01$, *** $p<0.001$

Figure 3. Co-dominance of RUNX3 and THPOK in DPT allows for the intermediate expression of CD4 and CD8 co-stimulatory proteins

(A) Schematic showing the relationship of RUNX3 and THPOK in CD8 and CD4 T cells. (B-D) Histograms of THPOK and RUNX3 (B) expression compared to an isotype that is further quantified (C-D). (E) Imagestream visualization of NKG2D expression on CD4, DP and CD8 T cells. (F) Analysis of 8 co-stimulatory markers on CD4, DP and CD8 T cells. Fold MFI represents

the median fluorescent intensity of the indicated marker divided by the median fluorescent intensity of an isotype control. * $p<0.05$

Figure 4. DPT are highly active and secrete both CD4 and CD8 lineage cytokines.
(A-B) T cells from the blood of GVHD mice were incubated overnight with PMA/ionomycin (A) or brefeldin A (B) prior to intracellular cytokine staining. (C) ATP production rate of the indicated flow-sorted T cell populations. (D) Representative dot plots of the indicated T cell population taken from a GVHD mouse. Boxes represent blasting T cells, a marker of activated and proliferating T cells. (E-F) Quantification of the percentage of T cells blasting from GVHD mice (E) and from thirteen allo-HSCT patients that developed ≥ grade 2 acute GVHD (F).

Figure 5. DPT are sufficient to mediate GVHD lethality after xenogeneic transplantation.
(A-D) Isolated CD4 and CD8 T cells from a healthy donor were transplanted into NSG mice and monitored for survival (B), GVHD score (C) and IFNγ concentration (D). (E-K) FACS sorted CD4, DPT and CD8 T cell populations were transplanted into NSG mice and monitored for survival (F), GVHD score (G) and IFNγ concentration (H). At the time of euthanasia, the number of T cells in target organs was quantified (I) and H&E histology performed and scored (J-K).

Figure 6. DPT do not possess direct GVL activity against human B-ALL.
(A-E) Kaplan-Meier survival curve (A) of NSG mice transplanted with the human B-ALL cancer line RS4;11 (black line) seven days prior to the transplantation of either DPT (red line) or PB-MNC (blue line). Mice were monitored for signs of pathology with mice given NT or DPT experiencing distinct pathology from PB-MNC. (B-D) Flow analysis (B) of mice given DPT and PB-MNC (C-D). T cell activation as measured by the concentration of IFNγ in the serum of mice (E). (F-J) Experiment was repeated using the luciferase positive human B-ALL cell line NALM-6 and freshy isolated CD4 and CD8 T cell from healthy donors along with DPTs. Kaplan-Meier survival curve (F) of the transplanted mice which all exhibited evidence of leukemia. Leukemic growth was confirmed using IVIS imaging (G-H) with flow cytometry to quantify the number of leukemia and T cells in the blood of mice across the indicated time points (I-J).

Figure 7. Presence of DPT in aGVHD Allo-HSCT Patients
Blood samples were collected from allo-HSCT patients either at the diagnosis of ≥ grade 2 aGVHD or between 70-90 days post-transplant. (A) Representative dot plots of a healthy human donor, an allo-HSCT patient with no signs of a GVHD at 82 days post-transplant and an allo-HSCT

554 patient that had active grade IV aGVHD at 84 days post-transplant. Red box indicates The
555 $CD4^+/CD8\beta^+$ DPT population. (B) Bar graph shows a total of 14 non-GVHD patients and 13 ≥
556 grade 2 aGVHD patient samples were collected. Each symbol indicates an individual patient. *
557 $p<0.05$, ** $p<.01$, *** $p<0.001$

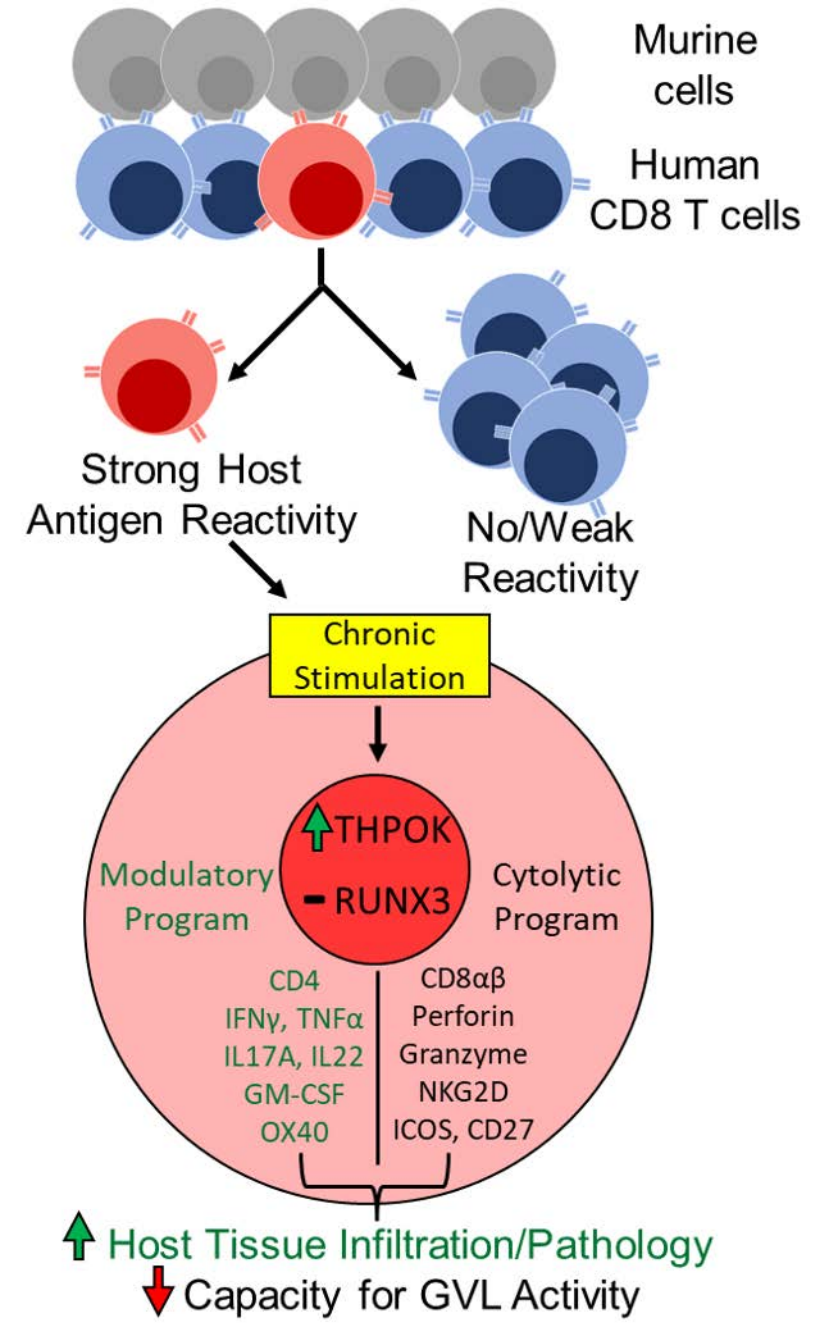

Visual Abstract

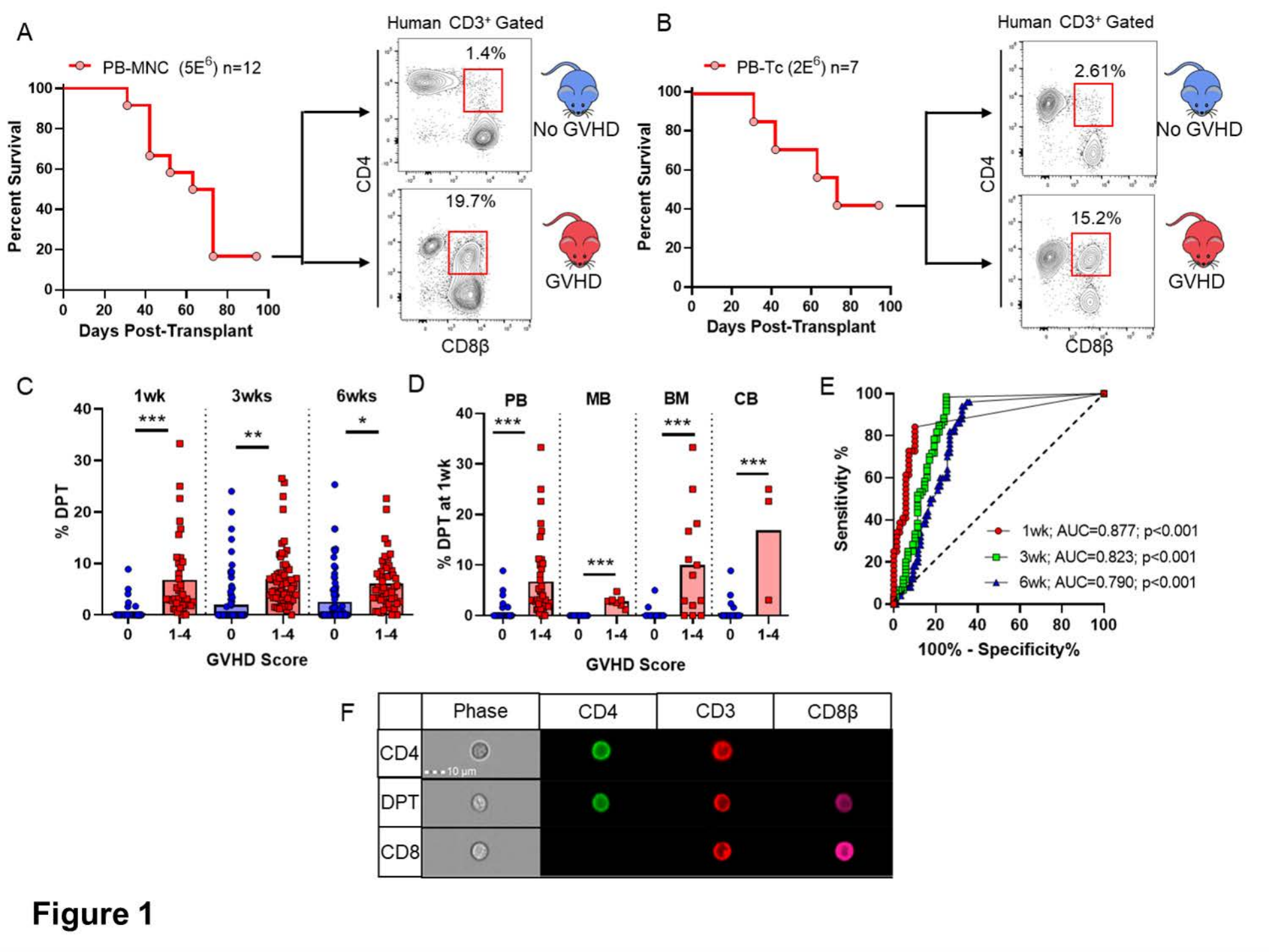
A
PB-MNC (5E6) n=12
Percent Survival
Days Post-Transplant
Human CD3+ Gated
1.4%
19.7%
CD4
CD8β
No GVHD
GVHD
B
PB-Tc (2E6) n=7
Percent Survival
Days Post-Transplant
Human CD3+ Gated
2.61%
15.2%
CD4
CD8β
No GVHD
GVHD
C
1wk
3wks
6wks
% DPT
GVHD Score
D
PB
MB
BM
CB
% DPT at 1wk
GVHD Score
E
Sensitivity %
100% - Specificity%
1wk; AUC=0.877; p<0.001
3wk; AUC=0.823; p<0.001
6wk; AUC=0.790; p<0.001
F
Phase
CD4
CD3
CD8β
CD4
DPT
CD8
10 µm

Figure 1

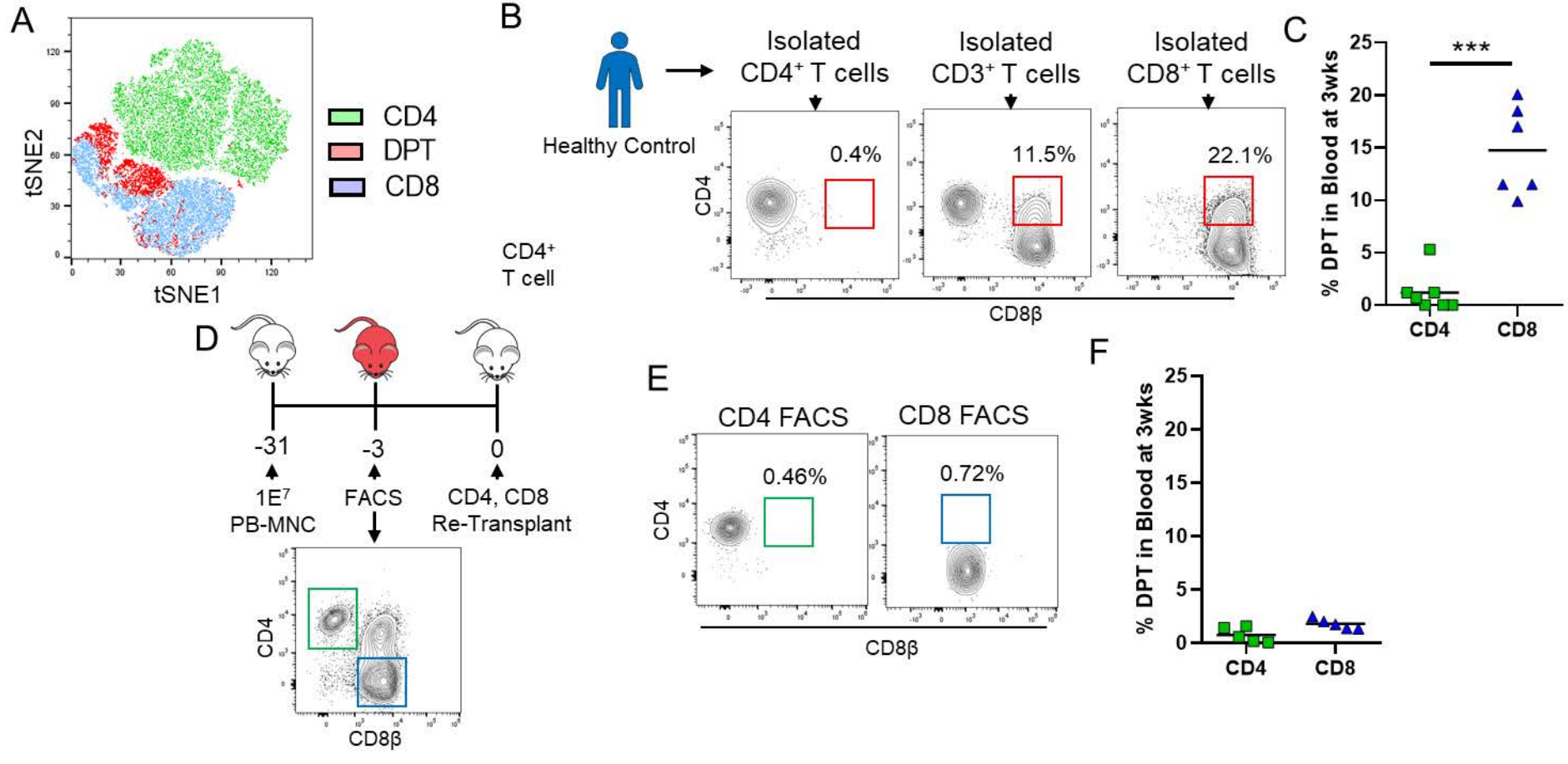
A
tSNE2
tSNE1
CD4
DPT
CD8
B
Healthy Control
Isolated CD4+ T cells
Isolated CD3+ T cells
Isolated CD8+ T cells
0.4%
11.5%
22.1%
CD4
CD8β
C
% DPT in Blood at 3wks
***
CD4
CD8
CD4+ T cell
D
-31
-3
0
1E7 PB-MNC
FACS
CD4, CD8 Re-Transplant
CD4
CD8β
E
CD4 FACS
CD8 FACS
0.46%
0.72%
CD4
CD8β
F
% DPT in Blood at 3wks
CD4
CD8

Figure 2

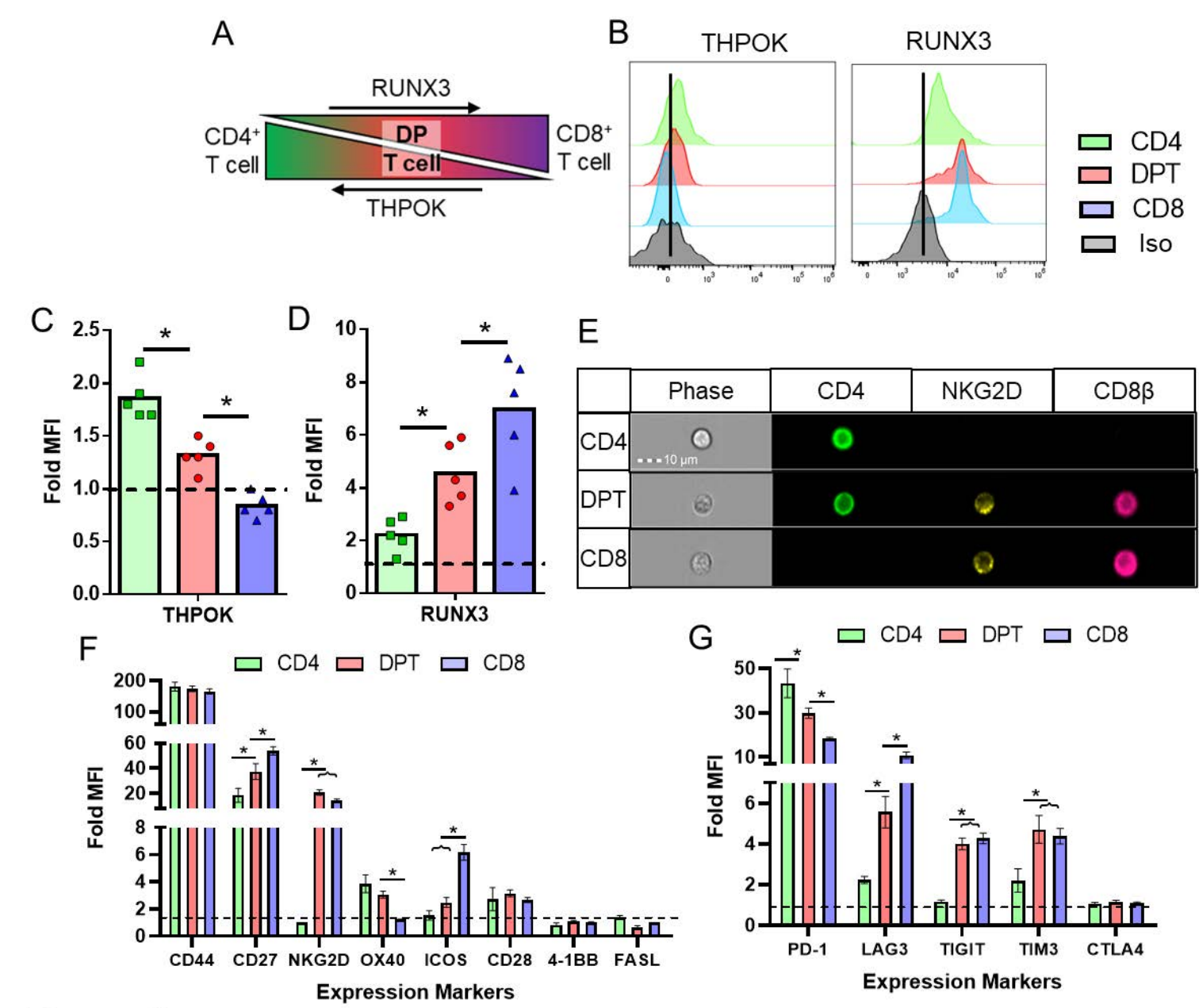
A
RUNX3
CD4+
T cell
DP
T cell
CD8+
T cell
THPOK
B
THPOK
RUNX3
CD4
DPT
CD8
Iso
C
Fold MFI
THPOK
D
Fold MFI
RUNX3
E
Phase
CD4
NKG2D
CD8β
CD4
DPT
CD8
10 μm
F
CD4
DPT
CD8
Fold MFI
CD44
CD27
NKG2D
OX40
ICOS
CD28
4-1BB
FASL
Expression Markers
G
CD4
DPT
CD8
Fold MFI
PD-1
LAG3
TIGIT
TIM3
CTLA4
Expression Markers

Figure 3

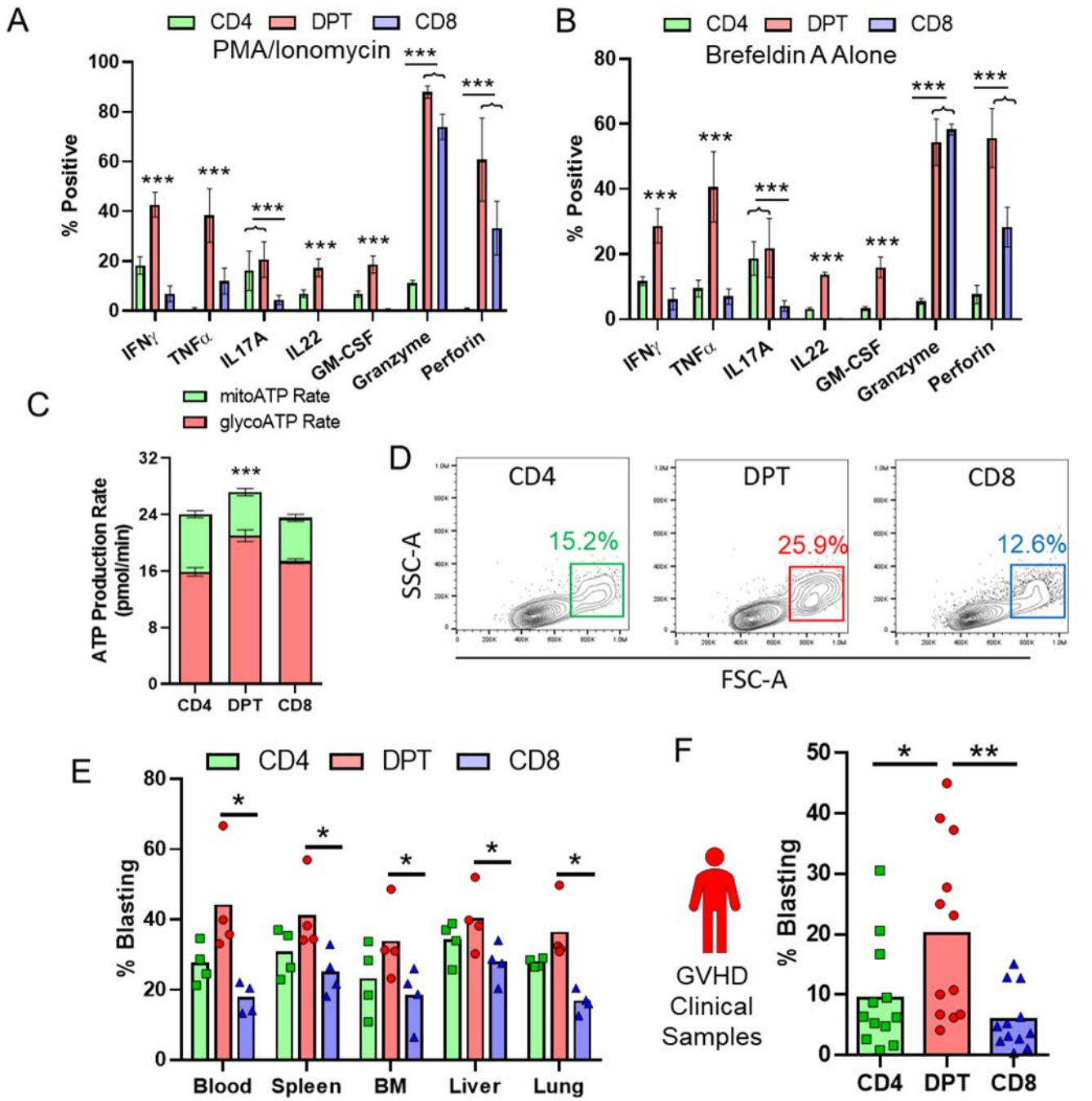
A
CD4
DPT
CD8
PMA/Ionomycin
% Positive
IFNγ
TNFα
IL17A
IL22
GM-CSF
Granzyme
Perforin
***
B
Brefeldin A Alone
C
mitoATP Rate
glycoATP Rate
ATP Production Rate (pmol/min)
D
SSC-A
FSC-A
15.2%
25.9%
12.6%
E
% Blasting
Blood
Spleen
BM
Liver
Lung
*
F
GVHD Clinical Samples
**

Figure 4

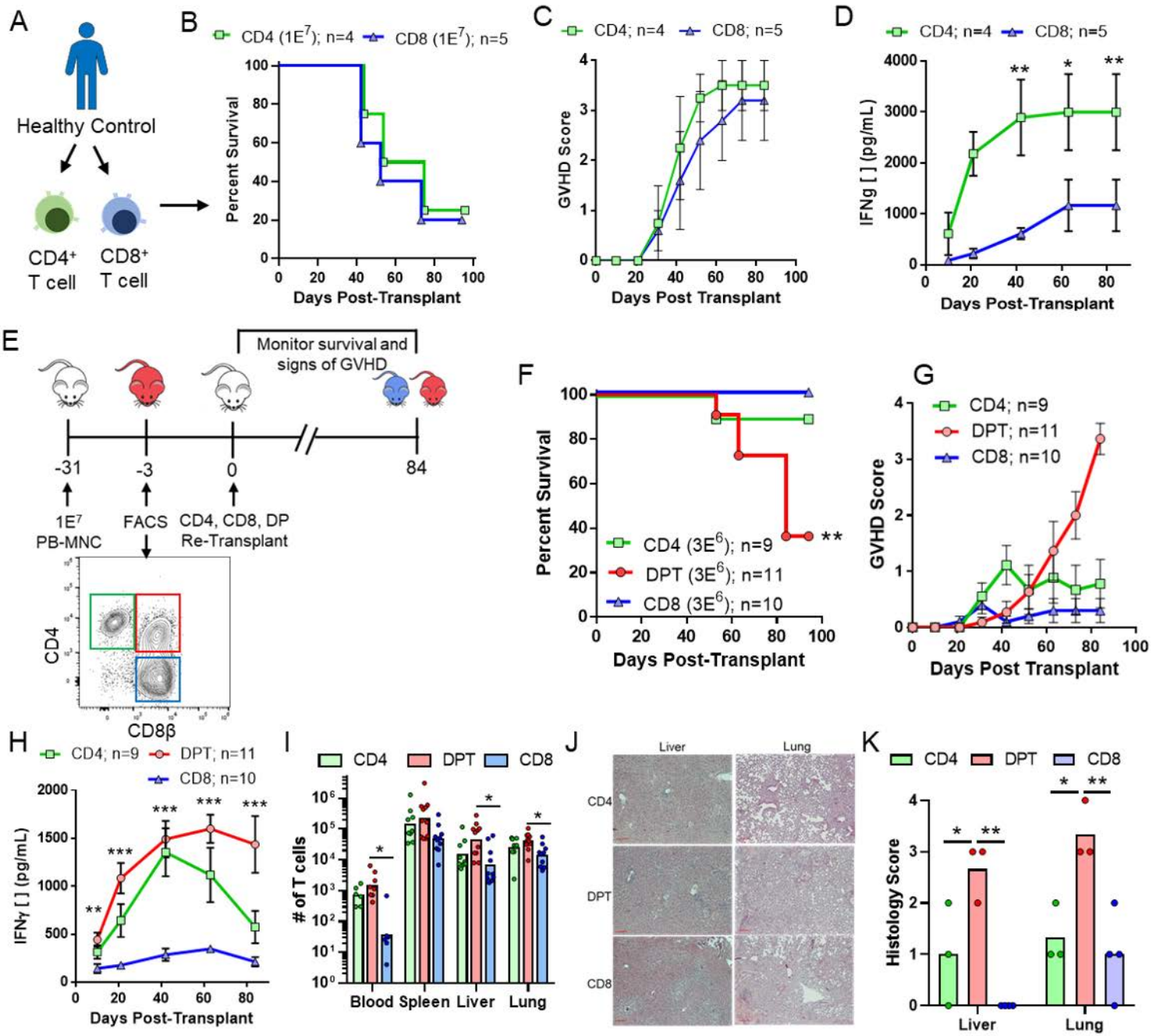
A
Healthy Control
CD4+ T cell
CD8+ T cell
B
CD4 (1E7); n=4
CD8 (1E7); n=5
Percent Survival
Days Post-Transplant
C
CD4; n=4
CD8; n=5
GVHD Score
Days Post Transplant
D
CD4; n=4
CD8; n=5
IFNg [ ] (pg/mL)
Days Post-Transplant
E
Monitor survival and signs of GVHD
-31
-3
0
84
1E7 PB-MNC
FACS
CD4, CD8, DP Re-Transplant
CD4
CD8β
F
Percent Survival
CD4 (3E6); n=9
DPT (3E6); n=11
CD8 (3E6); n=10
Days Post-Transplant
G
CD4; n=9
DPT; n=11
CD8; n=10
GVHD Score
Days Post Transplant
H
CD4; n=9
DPT; n=11
CD8; n=10
IFNγ [ ] (pg/mL)
Days Post-Transplant
I
CD4
DPT
CD8
# of T cells
Blood
Spleen
Liver
Lung
J
Liver
Lung
CD4
DPT
CD8
K
CD4
DPT
CD8
Histology Score
Liver
Lung

Figure 5

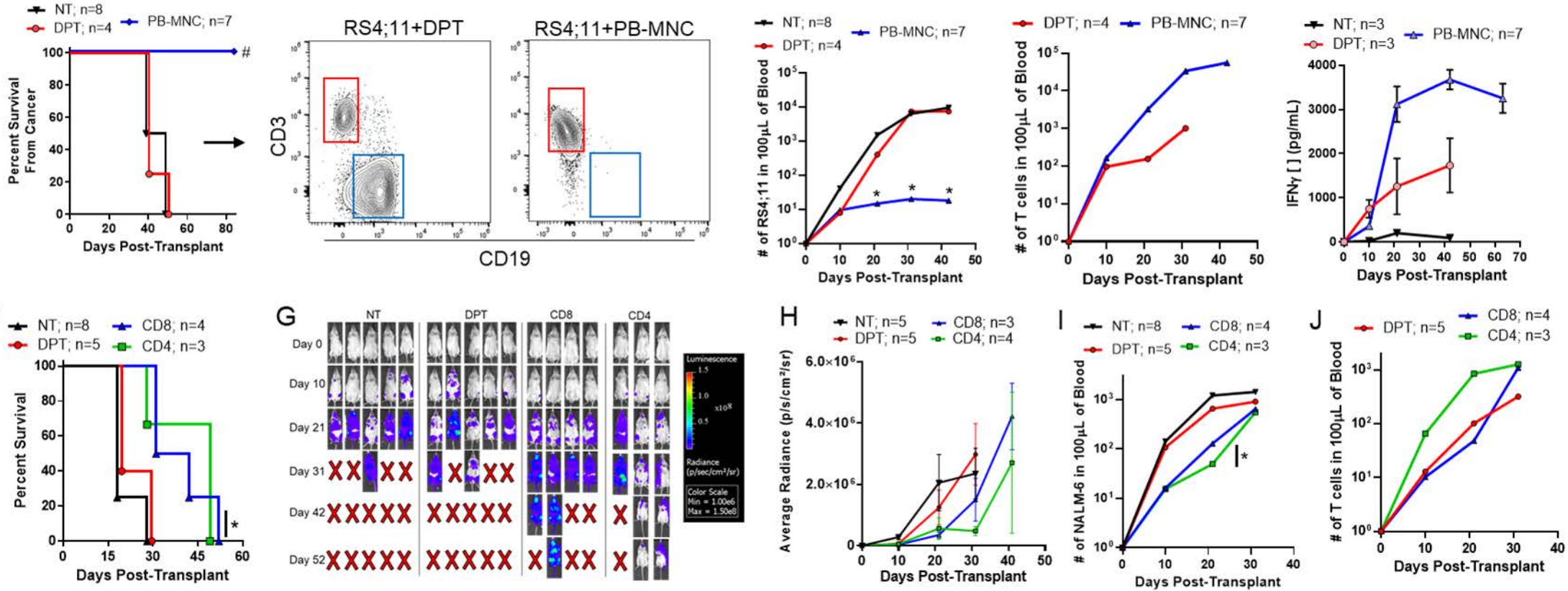
NT; n=8
DPT; n=4
PB-MNC; n=7
Percent Survival From Cancer
Days Post-Transplant
#
RS4;11+DPT
RS4;11+PB-MNC
CD3
CD19
# of RS4;11 in 100µL of Blood
# of T cells in 100µL of Blood
IFNγ [ ] (pg/mL)
NT; n=3
DPT; n=3
F
CD8; n=4
CD4; n=3
DPT; n=5
G
NT
DPT
CD8
CD4
Day 0
Day 10
Day 21
Day 31
Day 42
Day 52
Luminescence
Radiance (p/sec/cm²/sr)
Color Scale
Min = 1.00e6
Max = 1.50e8
H
NT; n=5
CD8; n=3
CD4; n=4
Average Radiance (p/s/cm²/sr)
I
# of NALM-6 in 100µL of Blood
J

Figure 6

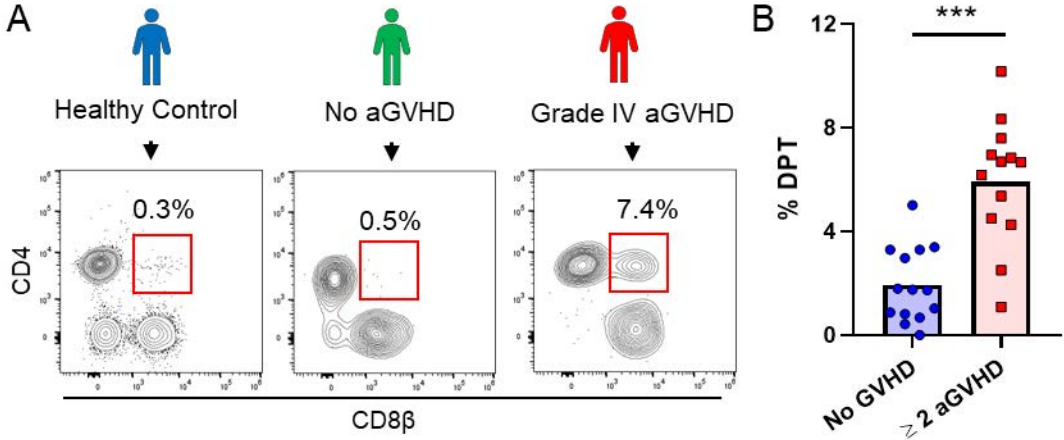
A
Healthy Control
No aGVHD
Grade IV aGVHD
0.3%
0.5%
7.4%
CD4
CD8β
B
***
% DPT
12
8
4
0
No GVHD
≥ 2 aGVHD

Figure 7